Macromolecules

ARTICLE

pubs.acs.org/Macromolecules

Vapor-Phase Free Radical Polymerization in the Presence of an Ionic Liquid

P. D. Haller, R. J. Frank-Finney, and M. Gupta*

Mork Family Department of Chemical Engineering and Materials Science, University of Southern California, Los Angeles, California 90089, United States

Supporting Information

ABSTRACT: An ionic liquid (IL) was introduced into a vapor-phase free radical polymerization process for the first time. The deposition of poly(2-hydroxyethyl methacrylate) (PHEMA) and poly(1*H*,1*H*,2*H*,2*H*-perfluorodecyl acrylate) (PPFDA) was studied in the presence of 1-butyl-3-methylimidazolium hexafluorophosphate ([bmim][PF_6]) droplets. The polymerization occurred either at the vapor−IL interface or within the IL depending on reaction conditions such as the duration of deposition, the stage temperature, and the monomer solubility. A variety of polymeric architectures such as polymer skins that completely encapsulated the droplet, free-standing polymer, and polymer films that float freely on the surface of the IL were formed. The results from this study will facilitate the design of new polymer−IL composite materials for use in fuel cell and battery applications.

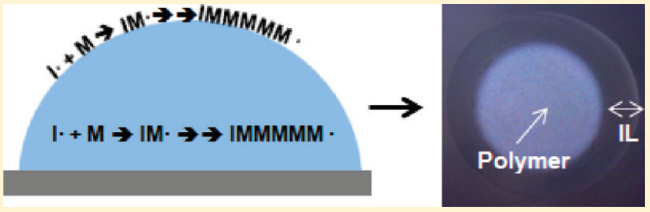

INTRODUCTION

Ionic liquids (ILs) are salts that are liquids at ambient temperatures. ILs have attracted significant interest as environmentally friendly alternatives to traditional volatile organic solvents because they are nonvolatile, nonflammable, and can be easily recycled.[1] Ionic liquids are both polar and noncoordinating solvents which can solvate a wide range of organic and inorganic reagents.[2,3] This unique combination of properties can be exploited in many ways to improve the selectivity and kinetics of chemical reactions,[4,5] including polymer synthesis.[6−8] For example, Hong et al. found that the free-radical polymerization of methyl methacrylate occurred 5 times faster in 1-butyl-3-methylimidazolium hexafluorophosphate ([bmim][PF_6]) than in benzene and resulted in polymers with 10 times higher molecular weights.[9] They proposed that the high viscosity of the ionic liquid and the precipitation of polymeric radicals caused a decrease in the rate of termination. In another example, Mays and coworkers synthesized block copolymers of poly(styrene) and poly(methyl methacrylate) (PST-*b*-PMMA) by synthesizing PST in 1-butyl-3-methylimidazolium hexafluorophosphate ([bmim][PF_6]) with an initiator, removing excess monomer and initiator, and then initiating the growth of PMMA chains from the living PST radicals.[10]

Because of their low volatility, ILs have recently been used in inorganic vacuum processes. For example, Borra et al.[11] fabricated a surface of high reflectivity by sputtering silver onto 1-ethyl-3-methylimidazolium ethylsulfate. They found that sputtering silver directly onto the surface of the IL led to a film consisting of colloidal particles, whereas sputtering a thin layer of chromium followed by silver led to a smooth film. In another example, Torimoto et al. found that sputtering gold onto the surface of ILs resulted in the formation of gold nanoparticles.[12] They found that the size of the nanoparticles depended on the IL used and the concentration of the nanoparticles depended on the duration of the sputtering process.

Although ILs have been used in inorganic vapor-phase deposition processes, we have not found examples of the use of ILs in organic vapor-phase deposition processes. In this paper, we introduce ILs into the initiated chemical vapor deposition (iCVD) process for the first time. The iCVD technique is a one-step, solventless process generally used to modify the surfaces of substrates with polymeric coatings.[13−15] The polymerization occurs via a free-radical mechanism, and the deposited polymeric coatings are structurally analogous to solution-phase polymers.[16] A kinetic model has been developed for the iCVD process that incorporates initiation, propagation, and termination as well as primary radical termination and recombination.[17] The iCVD process can be used to deposit a wide range of polymers, including poly(2-hydroxyethyl methacrylate) (PHEMA),[18] poly(4-vinylpyridine) (P4VP),[19] and poly(1*H*,1*H*,2*H*,2*H*-perfluorodecyl acrylate) (PPFDA).[20]

In this paper we combine the benefits of IL solvents and the iCVD process in a new system we call ILiCVD. We demonstrate that we can use the ILiCVD system to polymerize free-standing polymer, polymer skins that completely encapsulate the IL, and polymer films that float freely on the surface of the IL, depending on the reaction conditions. These polymer architectures cannot be formed using ILs or iCVD alone and are unique to our

Received: December 9, 2010
Revised: March 10, 2011
Published: March 24, 2011

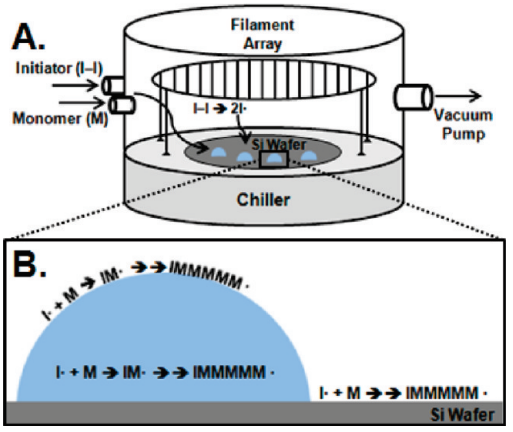

Figure 1. Schematic of the ILiCVD process. (A) Monomer molecules (M) and initiator radicals ($I^{\bullet}$) diffuse to the surface of a silicon substrate that contains IL droplets. (B) A magnified view showing that polymerization can occur at the vapor−IL interface, within the bulk IL, and at the vapor−silicon interface, depending on reaction conditions.

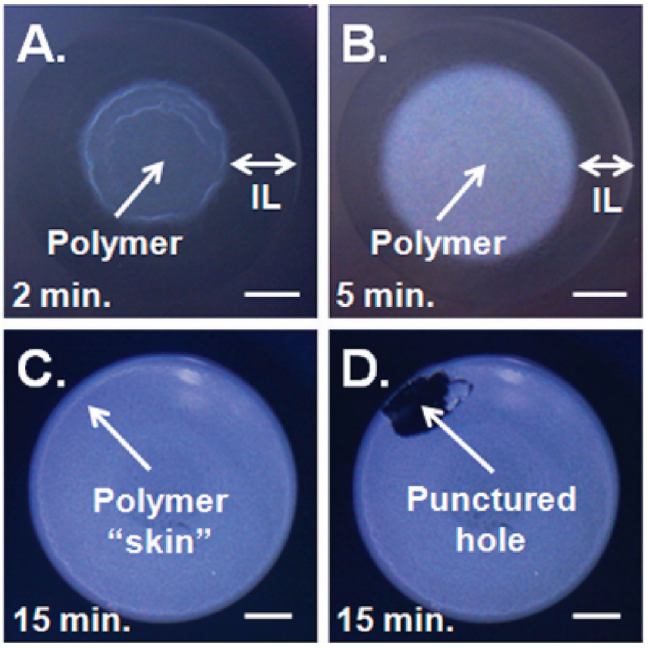

Figure 2. Images of PHEMA deposited onto a [bmim][PF_6] droplet at a stage temperature of 35 °C after (A) 2, (B) 5, and (C) 15 min. (D) After 15 min of PHEMA deposition, a polymer "skin" completely encapsulated the drop and a hole could be torn in the film. Scale bars represent 1 mm.

ILiCVD system. The mechanistic insight gained from our study will allow researchers to use the ILiCVD process to design polymer−IL composite materials for use as electrolyte membranes in fuel cells,[21,22] nonvolatile electrolytes in batteries,[23,24] and ionic liquid core−polymer shell particles for use in optical and chemical applications.[25,26]

RESULTS AND DISCUSSION

A schematic representation of the ILiCVD process is shown in Figure 1. Monomer and initiator vapors are introduced into the reaction chamber in which the initiator molecules are broken into

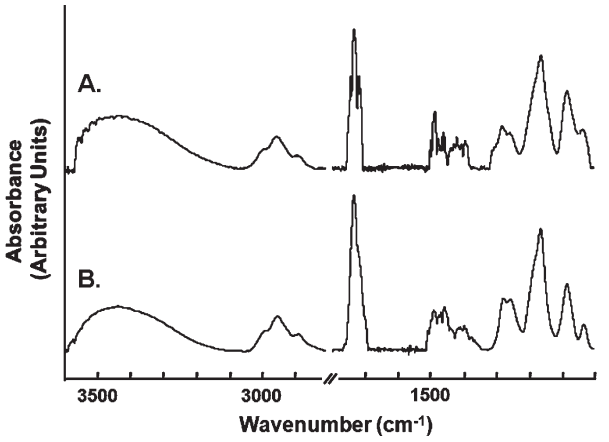

Figure 3. FTIR spectra of PHEMA films deposited using (A) iCVD and (B) ILiCVD.

radicals by the heated filament array and the reactants diffuse to the cooled substrate. The substrate consists of IL droplets on the surface of a silicon wafer. The polymerization can occur at the vapor−IL interface, within the IL, and at the vapor−silicon interface, depending on the reaction conditions. We studied the deposition of poly(2-hydroxyethyl methacrylate) (PHEMA) in the presence of 1-butyl-3-methylimidazolium hexafluorophosphate ([bmim][PF_6]) droplets as a function of time. The progression of the deposition of PHEMA at a stage temperature of 35 °C is shown in Figure 2. The PHEMA formed a thin continuous polymer film on top of the [bmim][PF_6] after 2 min (Figure 2A). This film was self-standing and could be lifted off of the [bmim][PF_6] droplet using a set of tweezers. The PHEMA film continued to grow after 5 min (Figure 2B). After 15 min, the polymer film completely encapsulated the [bmim][PF_6] droplet, forming a complete polymer skin (Figure 2C). To illustrate the continuous nature of this skin, a hole was torn into the skin using tweezers (Figure 2D).

The [bmim][PF_6] droplet spread over the course of the deposition process. For a 15 min deposition at 35 °C, a set of 5 droplets with initial diameters of 4.45 ± 0.53 mm spread to an average diameter of 6.30 ± 0.92 mm. The contact angle of [bmim][PF_6], and a PHEMA film and was found to be 35.7 ± 1.0° and 13.5 ± 0.7°, respectively. The spreading of the droplet during PHEMA deposition is therefore likely due to the increased attraction between the [bmim][PF_6] droplet and the PHEMA film formed on the silicon substrate surrounding the [bmim][PF_6] droplet. This hypothesis is supported by the presence of a polymer ring on the silicon substrate underneath the [bmim][PF_6] droplet. Furthermore, the inner diameter of the polymer ring matched the initial diameter of the [bmim][PF_6] droplet.

We used Fourier transform infrared spectroscopy (FTIR) to characterize the PHEMA films. Figure 3 compares the FTIR spectrum of a PHEMA film deposited on a silicon wafer using traditional iCVD and the spectrum of a PHEMA skin deposited on the [bmim][PF_6] droplet at a stage temperature of 35 °C using ILiCVD. The spectra are nearly identical, demonstrating that the films have the same composition. Both spectra have the expected major peaks: O−H stretching from 3600 to 3100 cm^{-1}, C−H stretching from 3050 to 2800 cm^{-1}, C═O stretching from 1770 to 1700 cm^{-1}, C−H bending from 1520 to 1350 cm^{-1}, and C−O stretching from 1310 to 1210 cm^{-1}.[18,27] The absence of

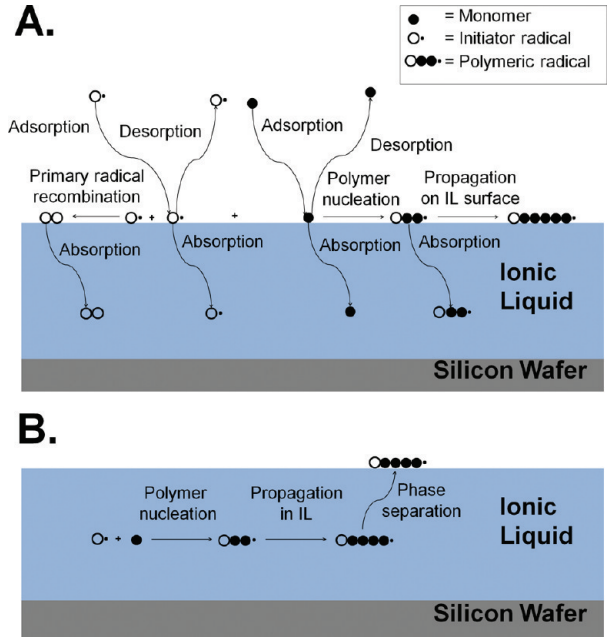

Figure 4. Expected reaction events occurring (A) at the vapor−IL interface and (B) within the IL.

additional peaks in the spectrum of the PHEMA film deposited by ILiCVD indicates the high purity of the polymer film.

PHEMA polymerization takes place simultaneously at both the vapor−[bmim][PF_6] interface and within the [bmim][PF_6]. The rate of polymerization at the interface is controlled by the diffusion of monomer molecules to the cooled substrate surface.[28] The temperatures at the vapor−[bmim][PF_6] interface and the vapor−silicon interface are similar, and therefore we expect similar deposition rates at both surfaces. Table S-1 in the Supporting Information shows the thicknesses of the PHEMA skins. The thickness at the edge of the skin is similar to the thickness of the PHEMA film on the silicon surface; however, the thickness at the center of the skin is significantly greater due to contributions from polymer chains that form within the bulk IL. Within 90 s of PHEMA deposition, there are polymer pieces floating at the center of the surface of the [bmim][PF_6] droplet. These polymer pieces form as HEMA monomer absorbs into the [bmim][PF_6] layer, and propagation occurs within the IL. At a critical molecular weight, the growing PHEMA chains become insoluble in the [bmim][PF_6] and float to the top because the density of PHEMA is lower (1.21 g/mL)[29] than that of [bmim][PF_6] (1.37 g/mL).[30] The increased thickness at the center of the PHEMA skins accounts for their rough appearance.

We investigated whether we could control the location of the polymerization by controlling the temperature of the stage. Figure 4 is a schematic representation of the proposed processes that occur at the vapor−IL interface (Figure 4A) and in the IL (Figure 4B). At the vapor−IL interface, the initiator radicals and monomer molecules can adsorb, desorb, react to form a polymer, or absorb into the IL. Figure 4B shows the processes that occur in the IL layer. Monomer and initiator radicals that have absorbed into the IL can react to form a polymer. Polymer can phase separate out of the bulk IL and float to the vapor−IL interface if the density of the polymer is less than that of the IL. Primary radical recombination can occur at the vapor−IL interface, but it is unlikely that the recombined species will form radicals in the IL due to the low temperature of the IL. Figure 4B does not show primary radical recombination or termination in the IL to demonstrate the expected low termination rates due to the viscosity of the IL.[31,32] We hypothesize that the concentration of the monomer at the vapor−IL interface will affect the location of the polymerization processes. In the iCVD process, the ratio of the monomer partial pressure (P_M) to the saturation pressure (P_{Sat}) governs the concentration of monomer at the interface between the vapor and solid. Increasing the stage temperature increases the saturation pressure and thereby decreases P_M/P_{Sat}. Decreasing P_M/P_{Sat} decreases the concentration of the monomer at the interface between the vapor and solid which leads to a decrease in the polymer deposition rate at the interface.[20] Figure 5 shows a comparison of the PHEMA depositions onto the [bmim][PF_6] droplets at stage temperatures of 35, 55, and 75 °C after 15 min. At a stage temperature of 35 °C, the deposition resulted in the formation of a polymer skin that completely encapsulated the [bmim][PF_6] droplet (Figure 5A). At this stage temperature, the concentration of HEMA monomer at the vapor−IL interface was high enough ($P_M/P_{Sat} \sim 0.25$) to cause fast polymerization at the interface relative to the IL which led to the formation of a continuous PHEMA skin.

At a stage temperature of 55 °C, a continuous polymer film was deposited onto the top surface of the [bmim][PF_6] droplet and a ring consisting of floating polymer pieces formed at the edge of the droplet (Figure 5B). At 55 °C, the concentration of HEMA monomer at the vapor−IL interface was high enough ($P_M/P_{Sat} \sim 0.06$) that polymerization was fast enough at the interface to form a continuous film but not fast enough to completely encapsulate the [bmim][PF_6] droplet in 15 min. The ring of floating polymer at the edge of the droplet is the result of the removal of low molecular weight polymer chains from the surface of the silicon. Gleason and co-workers showed that the molecular weight of polymers deposited by iCVD decreases with decreasing P_M/P_{Sat}.[28] Thus, the polymer deposited on the silicon at 55 °C has a lower molecular weight than the polymer deposited at 35 °C, and the force caused by the spreading of the [bmim][PF_6] droplet during deposition was sufficient to remove the low molecular weight polymer from the surface of the silicon. To test this hypothesis, we placed [bmim][PF_6] droplets onto PHEMA films that were previously deposited at stage temperatures of 35 and 55 °C. The droplets placed on the film deposited at 35 °C spread but did not remove polymer from the surface of the silicon, whereas the droplets placed on the film deposited at 55 °C spread and removed some polymer from the surface of the silicon. We also tested our hypothesis by first placing [bmim][PF_6] droplets onto a PHEMA film previously deposited at 35 °C and then allowing the droplets to spread. Next, we conducted a PHEMA deposition onto the droplet at 55 °C. A continuous PHEMA film was deposited on the surface of the [bmim][PF_6], but there was no ring present because the drops did not spread further during the deposition.

Deposition at a stage temperature of 75 °C led to the formation of polymer pieces floating on the [bmim][PF_6] droplets (Figure 5C). At this stage temperature, the concentration of HEMA monomer at the vapor−IL interface was very low ($P_M/P_{Sat} \sim 0.02$). There was no visible deposition on the silicon substrate surrounding the IL droplet at a stage temperature of 75 °C, whereas there was PHEMA deposition on the silicon substrate at stage temperatures of 35 and 55 °C. Since there was no polymer deposition at the vapor−silicon interface at 75 °C,

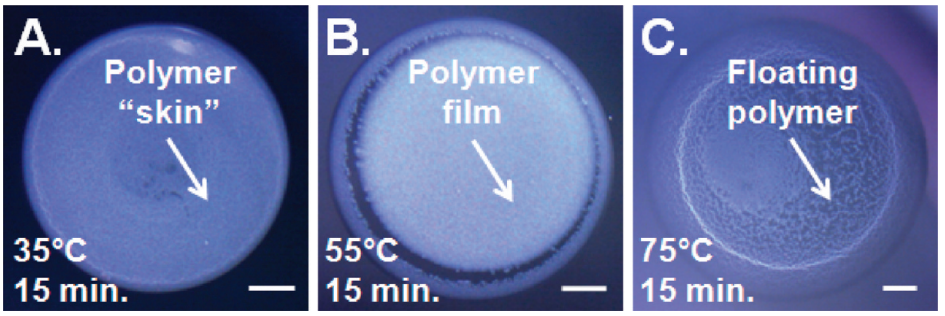

Figure 5. Images of PHEMA deposited onto a [bmim][PF_6] droplet after 15 min at stage temperatures of (A) 35, (B) 55, and (C) 75 °C. Scale bars represent 1 mm.

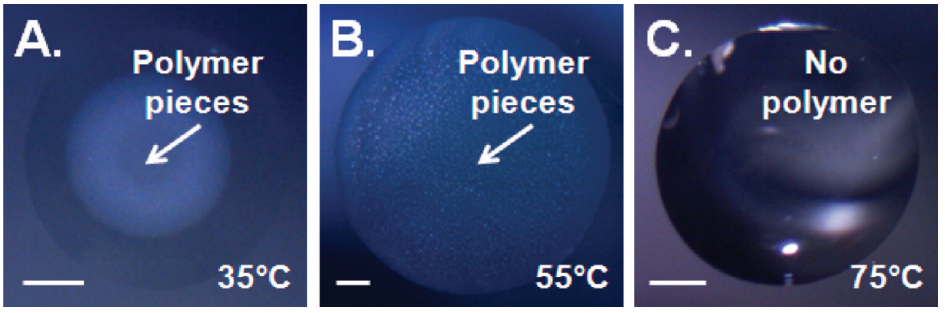

Figure 6. Images of PHEMA deposited after saturating the [bmim][PF_6] with HEMA monomer and subsequently flowing initiator at a stage temperature of (A) 35, (B) 55, and (C) 75 °C. Scale bars represent 1 mm.

we do not expect that there will be formation of polymer at the vapor−IL interface. We therefore hypothesize that the floating polymer pieces in Figure 5C are formed within the [bmim][PF_6] and not at the vapor−IL interface. The PHEMA chains float to the top of the [bmim][PF_6] droplet as they grow and become immiscible, similar to the 90 s PHEMA deposition at a stage temperature of 35 °C.

In the iCVD process, the monomer and initiator vapors flow simultaneously and continuously throughout the deposition. The sequential flow of monomer vapor followed by initiator vapor does not lead to polymerization because the monomer molecules will not stay adsorbed to the surface of the substrate and instead will be pumped out of the system before the introduction of the initiator vapor. In the ILiCVD process, however, the IL can act as a monomer trap. The IL can hold the monomer molecules after the flow of monomer vapor has been stopped and excess monomer vapor has been pumped out of the reactor. When initiator vapor is flowed into the system, polymerization can only occur within the IL in which monomer molecules are trapped. To test our hypothesis, HEMA monomer and initiator vapors were flowed into the reactor for 15 min at a stage temperature of 35 °C, without turning on the filament. This allowed the HEMA molecules to absorb into the [bmim][PF_6] without reacting. The reactor was then pumped down for 15 min to remove excess monomer vapor. Initiator vapor was then introduced into the reactor for 15 min with the filament array turned on but without the introduction of additional monomer. The sequential flow of HEMA and initiator at a stage temperature of 35 °C led to the formation of floating PHEMA polymer pieces (Figure 6). There was no polymerization on the surrounding silicon. The formation of polymer pieces instead of a continuous film is to be expected since polymerization can only occur within the [bmim][PF_6] in which monomer molecules are trapped. The similarity in the polymer architectures between Figure 6A and Figure 5C further validates our hypothesis that the PHEMA polymerization at a stage temperature of 75 °C occurred within the [bmim][PF_6] and not at the vapor−IL interface. We ran depositions using the same sequential monomer and initiator flow conditions at stage temperatures of 55 and 75 °C. PHEMA polymer pieces were synthesized at a stage temperature of 55 °C (Figure 6B), but there was no visible polymerization at a stage temperature of 75 °C (Figure 6C). One possible explanation for the lack of polymerization at 75 °C is that less HEMA monomer was absorbed into the [bmim][PF_6] at higher stage temperatures.

We tested the absorption of HEMA monomer into [bmim][PF_6] droplets as a function of time at stage temperatures of 35, 55, and 75 °C by flowing monomer and initiator without turning on the filament array. Figure S-1 in the Supporting Information shows that at a constant substrate temperature the contact angle decreased with increasing absorption time before reaching a minimum contact angle. The minimum contact angle decreased with decreasing stage temperature and was 20.3 ± 1.2°, 28.1 ± 1.0°, and 31.6 ± 0.9° at stage temperatures of 35, 55, and 75 °C, respectively. In order to verify that the lower contact angle at 35 °C indicates more absorption of monomer, we made mixtures of HEMA monomer and [bmim][PF_6] and tested their contact angles. Pure [bmim][PF_6] had a contact angle of 35.7 ± 1.0° on silicon. The contact angles were 30.6 ± 1.1° at 16:1 (volume of [bmim][PF_6]:volume of HEMA), 23.2 ± 1.4° at 8:1, 21.6 ± 1.0° at 2:1, 14.8 ± 1.4° at 1:1, and 9.0 ± 0.7° at 0:1 (pure HEMA monomer). We can conclude that the contact angle decreases with increasing monomer concentration in the [bmim][PF_6] and the decreased contact angle at 35 °C indicates

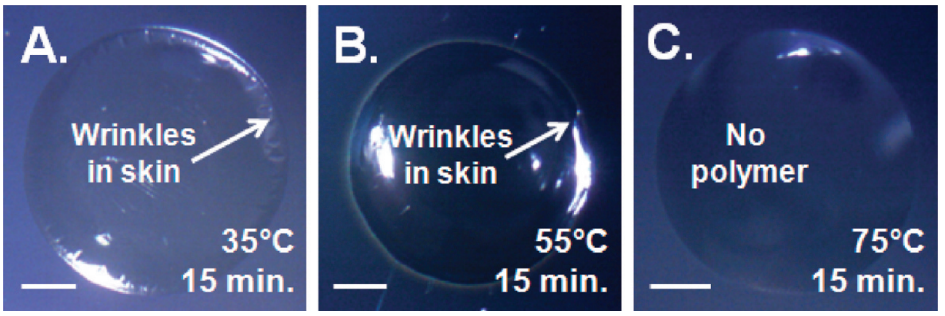

Figure 7. Images of PPFDA deposited onto a [bmim][PF_6] droplet after 15 min at stage temperatures of (A) 35, (B) 55, and (C) 75 °C. Scale bars represent 1 mm.

higher monomer absorption at lower stage temperatures. To quantify the amount of HEMA monomer absorbed in 60 min, the mass of the IL was measured before and after absorption. The amounts of HEMA absorbed were 34, 19, and 5 vol % at stage temperatures of 35, 55, and 75 °C, respectively. The temperature dependence of absorption was further confirmed by FTIR analysis. Figure S-2 in the Supporting Information shows the spectra of the [bmim][PF_6] after HEMA absorption trials of 60 min. The spectra have peaks at 1710 cm^{-1} due to the C═O stretching of the HEMA monomer, the magnitude of which decreased as the stage temperature increased. We note that the ability to use the sequential flow of monomer and initiator to polymerize within the IL layer will only work with monomers that are soluble within the IL.

We also studied the deposition of poly(1*H*,1*H*,2*H*,2*H*-perfluorodecyl acrylate) (PPFDA) in order to determine the effect of monomer solubility on the ILiCVD process. Whereas the HEMA monomer is soluble in [bmim][PF_6], the PFDA monomer is insoluble in [bmim][PF_6]. It has been shown that 1,3-dialkylimidazolium ILs have a supramolecular structure based on hydrogen bonding between the cation and the anion.[33,34] We believe that the PFDA monomer does not dissolve in [bmim][PF_6] because it does not contain any donor groups for hydrogen bonding and therefore cannot contribute to the supramolecular structure of the [bmim][PF_6]. Furthermore, Kubisa et al. showed that acrylate solubility decreases in [bmim][PF_6] as the size of the acrylate increases.[35] Since the PFDA monomer cannot absorb into the [bmim][PF_6], the PPFDA polymer cannot form within the [bmim][PF_6] and can only form at the vapor−[bmim][PF_6] interface. We studied the deposition of PPFDA as a function of time at a stage temperature of 35 °C and found that PPFDA skins that completely encapsulated the [bmim][PF_6] droplets formed within 2 min. In order to determine the effect of stage temperature, we tested the deposition of PPFDA at stage temperatures of 35, 55, and 75 °C. Figure 7 shows PPFDA deposited onto a [bmim][PF_6] droplet after 15 min. At a stage temperature of 35 °C, the concentration of PFDA monomer at the vapor−IL interface was high enough ($P_M/P_{Sat} \sim 0.27$) that polymerization occurred at the vapor−IL interface and a continuous PPFDA skin formed (Figure 7A). At a stage temperature of 55 °C ($P_M/P_{Sat} \sim 0.09$), a continuous PPFDA skin also formed (Figure 7B). At a stage temperature of 75 °C, there was no skin formation because the concentration of PFDA monomer at the vapor−IL interface was very low ($P_M/P_{Sat} \sim 0.03$) and there was no polymerization within the [bmim][PF_6] since the PFDA monomer is insoluble (Figure 7C).

Unlike the PHEMA case, the [bmim][PF_6] droplet slightly contracted during PPFDA deposition. A set of 5 droplets had an average diameter of 5.16 ± 0.38 mm before a 15 min deposition at a stage temperature of 35 °C and an average diameter of 4.88 ± 0.36 mm after the deposition. The contact angles of [bmim][PF_6] on silicon and a PPFDA film were found to be 35.7 ± 1.0° and 95.2 ± 0.8°, respectively. The contraction of the droplet during PPFDA deposition is likely due to the decreased wetting between the [bmim][PF_6] droplet and the PPFDA film that was deposited on the surrounding silicon.

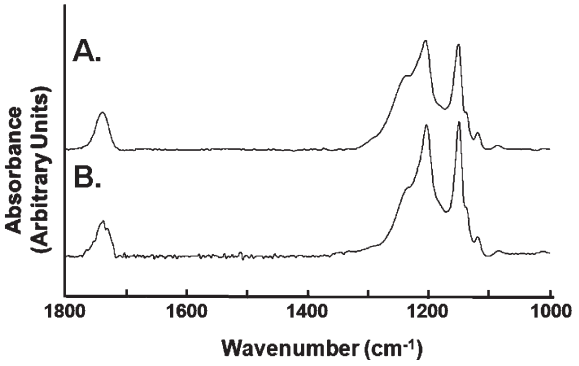

Figure 8. FTIR spectra of PPFDA films deposited using (A) iCVD and (B) ILiCVD.

We used FTIR spectroscopy to characterize the PPFDA films deposited at a stage temperature of 35 °C. Figure 8 compares the FTIR spectra of a PPFDA film deposited onto a silicon wafer using traditional iCVD and a PPFDA skin deposited onto a [bmim][PF_6] droplet using ILiCVD. The spectra are nearly identical, demonstrating that the films have the same composition. Both spectra have the expected major peaks: C═O stretching at 1741 cm^{-1}, asymmetric CF_2 stretching at 1242 cm^{-1}, symmetric CF_2 stretching at 1207 cm^{-1}, and a CF_2CF_3 peak at 1153 cm^{-1}.[20] The absence of additional peaks in the spectrum of the PPFDA film deposited using ILiCVD indicates the high purity of the polymer film.

In contrast to the PHEMA skins, the PPFDA skins have a more uniform thickness as shown in Table S-2 of the Supporting Information. This suggests that PPFDA polymerization begins evenly across the vapor−IL interface. The thickness of the skins is the same as the thickness of the PPFDA film on the silicon surface, confirming that the deposition rate is the same at the vapor−IL interface and at the silicon−vapor interface.

CONCLUSIONS

This work demonstrates the vapor-phase deposition of polymers in the presence of ILs for the first time. The ILiCVD process

is environmentally benign because organic solvents are not used in the process. The combined ILiCVD system can be used to polymerize free-standing polymer, polymer skins that completely encapsulate the IL, and polymer films that float freely on the IL surface. The nature of the deposited polymer depends on the deposition time, the stage temperature, and the solubility of the monomer in the IL. This level of control is not possible in solution-phase processes and can be utilized to develop composite polymer−IL materials with controlled structures. The wide variety of monomers and ILs will enable us to tailor highly specific combinations of polymer solubility, functionality, ionic conductivity, and other properties of composite materials using the ILiCVD system. These materials could potentially be used as electrolyte membranes in fuel cells, nonvolatile electrolytes in batteries, or as ionic liquid core−polymer shell particles in optical and chemical applications. Polymer−IL composite materials have attracted interest for use as electrolyte membranes in fuel cells.[36−38] Owing to their high thermal stability, these polymer−IL composite materials could enable the development of fuel cells that operate above 100 °C, which will improve electrode kinetics, increase carbon monoxide tolerance in the catalyst, and reduce the difficulty associated with controlling water content in current electrolyte systems.[39] However, the conductivity of these materials must be increased in order to compete with existing technologies.[21] One way to increase the conductivity of these materials is to increase the IL content.[38] The extension of our work to additional polymers and ILs may enable the development of polymer−IL composite materials with high IL content for improved conductivity.

EXPERIMENTAL SECTION

The 1-butyl-3-methylimidazolium hexafluorophosphate ([bmim][PF_6]) ionic liquid (97%, Aldrich), 2-hydroxyethyl methacrylate (HEMA) monomer (98%, Aldrich), 1*H*,1*H*,2*H*,2*H*-perfluorodecyl acrylate (PFDA) monomer (97%, Aldrich), and *tert*-butyl peroxide (TBPO) initiator (98%, Aldrich) were used without further purification. Ionic liquid droplets (5 μL) were dispensed from a micropipet onto 4 in. silicon wafers which were placed into a custom designed reaction chamber (250 mm diameter, 48 mm height). A nichrome filament array (80% Ni, 20% Cr, Omega Engineering) was resistively heated to 200 °C, and the distance between the filament array and the substrate was kept constant at 32 mm. The reactor stage was backside cooled to 35, 55, or 75 °C using a recirculating chiller. For poly(2-hydroxyethyl methacrylate) (PHEMA) depositions, the HEMA monomer was heated to 55 °C in a jar and flowed into the reactor at a rate of 0.52 sccm. TBPO was kept at room temperature and flowed into the reactor at a rate of 2.52 sccm, and the reactor pressure was maintained at 0.50 Torr. For poly(1*H*,1*H*,-2*H*,2*H*-perfluorodecyl acrylate) (PPFDA) depositions, the PFDA monomer was heated to 50 °C and flowed into the reactor at a rate of 0.28 sccm, TBPO was kept at room temperature and flowed into the reactor at a rate of 3.30 sccm, and the reactor pressure was maintained at 0.35 Torr.

The droplets of [bmim][PF_6] were imaged using a stereo microscope at 10× total magnification. The thickness of the polymer skins was determined using a JEOL-6610 low-vacuum scanning electron microscope. Ionic liquid was removed from the droplets by puncturing the skin near the edge and using compressed air to force the IL though the hole. The silicon substrate underneath the skin was cracked and mounted in a substrate holder such that the cross-section could be visualized. A thin gold coating was sputtered onto the surface of the sample before imaging. Film thicknesses on silicon were determined using a profilometer (Ambios Technology XP-2 stylus profilometer). Fourier transform infrared spectroscopy (FTIR) (Thermo Nicolet iS10) was used to study the chemical composition of the PHEMA and PPFDA films. The polymer was removed from the surface of the [bmim][PF_6] drops using forceps and rinsed with methanol before analysis. Contact angle goniometry (ramé-hart Model 290-F1) was used to study surface interactions. For the absorption trials, the contact angle was measured immediately after absorption by removing the sample from the reactor and transferring the IL to a clean silicon substrate. For all contact angle measurements, drops (5 μL) were allowed to equilibrate for 5 min before static contact angles were measured.

ASSOCIATED CONTENT

Supporting Information. Figures S-1 and S-2 and Tables S-1 and S-2. This material is available free of charge via the Internet at http://pubs.acs.org.

AUTHOR INFORMATION

Corresponding Author
*E-mail: malanchg@usc.edu.

ACKNOWLEDGMENT

This material is based on work supported by the National Science Foundation under Grant No. EEC-0310723 and the James H. Zumberge Faculty Research and Innovation Fund.

REFERENCES

(1) Holbrey, J. D.; Seddon, K. R. *Clean Prod. Process.* **1999**, *1*, 223–236.
(2) Welton, T. *Chem. Rev.* **1999**, *99*, 2071–2083.
(3) Miao, W.; Chan, T. H. *Acc. Chem. Res.* **2006**, *39*, 897–908.
(4) Carmichael, A. J.; Earle, M. J.; Holbrey, J. D.; McCormac, P. B.; Seddon, K. R. *Org. Lett.* **1999**, *1*, 997–1000.
(5) Sheldon, R. *Chem. Commun.* **2001**, *37*, 2399–2407.
(6) Sarbu, T.; Matyjaszewski, K. *Macromol. Chem. Phys.* **2001**, *202*, 3379–3391.
(7) Kubisa, P. *J. Polym. Sci., Part A: Polym. Chem.* **2005**, *43*, 4675–4683.
(8) Winterton, N. *J. Mater. Chem.* **2006**, *16*, 4281–4293.
(9) Hong, K.; Zhang, H.; Mays, J. W.; Visser, A. E.; Brazel, C. S.; Holbrey, J. D.; Reichert, W. M.; Rogers, R. D. *Chem. Commun.* **2002**, *38*, 1368–1369.
(10) Zhang, H.; Hong, K.; Mays, J. W. *Macromolecules* **2002**, *35* 5738–5741.
(11) Borra, E. F.; Seddiki, O.; Angel, R.; Eisenstein, D.; Hickson, P.; Seddon, K. R.; Worden, S. P. *Nature* **2007**, *447*, 979–981.
(12) Torimoto, T.; Okazaki, K.; Kiyama, T.; Hirahara, K.; Tanaka, N.; Kuwabata, S. *Appl. Phys. Lett.* **2006**, *89*, 243117.
(13) Ma, M.; Mao, Y.; Gupta, M.; Gleason, K. K.; Rutledge, G. G. *Macromolecules* **2005**, *38*, 9742–9748.
(14) Gupta, M.; Kapur, V.; Pinkterton, N. M.; Gleason, K. K. *Chem. Mater.* **2008**, *20*, 1646–1651.
(15) Lau, K. K. S.; Gleason, K. K. *Adv. Mater.* **2006**, *18*, 1972–1977.
(16) Tenhaeff, W. E.; Gleason, K. K. *Adv. Funct. Mater.* **2008**, *18*, 979–992.
(17) Lau, K. K. S.; Gleason, K. K. *Macromolecules* **2006**, *39*, 3695–3703.
(18) Chan, K.; Gleason, K. K. *Langmuir* **2005**, *21*, 8930–8939.
(19) Tenhaeff, W. E.; McIntosh, L. D.; Gleason, K. K. *Adv. Funct. Mater.* **2010**, *20*, 1144–1151.
(20) Gupta, M.; Gleason, K. K. *Langmuir* **2006**, *22*, 10047–10052.
(21) Steele, B. C. H.; Heinzel, A. *Nature* **2001**, *414*, 345–352.
(22) Armand, M.; Endres, F.; MacFarlane, D. R.; Ohno, H.; Scrosati, B. *Nature Mater.* **2009**, *8*, 621–629.
(23) Noda, A.; Watanabe, M. *Electrochim. Acta* **2000**, *45*, 1265–1270.

(24) Seki, S.; Kobayashi, Y.; Miyashiro, H.; Ohno, Y.; Usami, A.; Mita, Y.; Kihira, N.; Watanabe, M.; Terada, N. *J. Phys. Chem. B* **2006**, *110*, 10228–10230.
(25) Yow, H. N.; Routh, A. F. *Soft Matter* **2006**, *2*, 940–949.
(26) Sivakumar, S.; Bansal, V.; Cortez, C.; Chong, S.-F.; Zelikin, A. N.; Caruso, F. *Adv. Mater.* **2009**, *21*, 1820–1824.
(27) Perova, T. S.; Vij, J. K.; Xu, H. *Colloid Polym. Sci.* **1997**, *275*, 323–332.
(28) Lau, K. K. S.; Gleason, K. K. *Macromolecules* **2006**, *39*, 3688–3694.
(29) Diego, R. B.; Olmedilla, M. P.; Aroca, Á. S.; Ribelles, J. L. G.; Pradas, M. M.; Ferrer, G. G.; Sánchez, M. S. *J. Mater. Sci.* **2005**, *40*, 4881–4887.
(30) Troncoso, J.; Cerdeiriña, C. A.; Sanmamed, Y. A.; Romaní, L.; Rebelo, L. P. N. *J. Chem. Eng. Data* **2006**, *51*, 1856–1859.
(31) Schmidt-Naake, G.; Woecht, I.; Schmalfuβ, A. *Macromol. Symp.* **2007**, *259*, 226–235.
(32) Andrzejewska, E.; Podgorska-Golubska, M.; Stepniak, I.; Andrzejewski, M. *Polymer* **2009**, *50*, 2040–2047.
(33) Consorti, C. S.; Suarez, P. A. Z.; de Souza, R. F.; Burrow, R. A.; Farrar, D. H.; Lough, A. J.; Loh, W.; da Silva, L. H. M.; Dupont, J. *J. Phys. Chem. B* **2005**, *109*, 4341–4349.
(34) Kaar, J. L.; Jesionowski, A. M.; Berberich, J. A.; Moulton, R.; Russell, A. J. *J. Am. Chem. Soc.* **2003**, *125*, 4125–4131.
(35) Biedroń, T.; Kubisa, P. *Macromol. Rapid Commun.* **2001**, *22*, 1237–1242.
(36) Fuller, J.; Breda, A. C.; Carlin, R. T. *J. Electroanal. Chem.* **1998**, *459*, 29–34.
(37) Susan, M. A. B. H.; Kaneko, T.; Noda, A.; Watanabe, M. *J. Am. Chem. Soc.* **2005**, *127*, 4976–4983.
(38) Martinelli, A.; Matic, A.; Jacobsson, P.; Börjesson, L.; Fernicola, A.; Panero, S.; Scrosati, B.; Ohno, H. *J. Phys. Chem. B* **2007**, *111*, 12462–12467.
(39) Li, Q.; He, R.; Jensen, J. O.; Bjerrum, N. J. *Chem. Mater.* **2003**, *15*, 4896–4915.